https://doi.org/10.5194/hess-2021-48
Preprint. Discussion started: 4 February 2021

Hydrology and Earth System Sciences
Discussions

Climatic expression of rainfall on soil moisture dynamics in drylands

Isaac Kipkemoi[1], Katerina Michaelides[1,2,3], Rafael Rosolem[3,4], Michael Bliss Singer [2,5,6]

[1]School of Geographical Sciences, University of Bristol, Bristol, BS8 1SS, UK
[2]Earth Research Institute, University of California Santa Barbara, Santa Barbara, California 91306, USA
[3]Cabot Institute, University of Bristol, BS8 1UH, UK
[4]Faculty of Engineering, University of Bristol, Bristol, BS8 1TR, UK
[5]School of Earth and Ocean Sciences, Cardiff University, Cardiff, CF10 3AT, UK
[6]Water Research Institute, Cardiff University, Cardiff, CF10 3AX, UK

Correspondence to: ik17250@bristol.ac.uk & katerina.michaelides@bristol.ac.uk

Abstract. In drylands, characterised by water scarcity and frequent meteorological droughts, knowledge of soil moisture dynamics and its drivers (evapotranspiration, soil physical properties and the timing and sequencing of precipitation events) is fundamental to understanding changes in water availability to plants and human society, especially under a nonstationary climate. Given the episodic and stochastic nature of rainfall in drylands and the limited availability of data in these regions, we sought to explore what effects the temporal resolution of precipitation data has on soil moisture and how soil moisture distributions might evolve under different scenarios of climate change. Such information is critical for anticipating the impact of a changing climate on dryland communities across the globe, especially those that depend on rainfed agriculture and groundwater wells for drinking water for humans and livestock. A major challenge to understanding soil moisture in response to climate is the availability of precipitation datasets for dryland regions across the globe. Gridded precipitation data may only be available for daily or weekly time periods, even though rainstorms in drylands often occur on much shorter time scales, but it is currently unknown how this timescale mismatch might affect our understanding of soil moisture. Numerical modelling enables retrodiction or prediction of how climate translates into dynamically evolving moisture within the soil profile. It can be used to explore how climate data at different temporal resolutions affect these soil moisture dynamics, as well as to explore the influence of shifts in rainfall characteristics (e.g., storm intensity) under potential scenarios of climate change. This study uses Hydrus 1-D, to investigate the dynamics of soil moisture over a period of decades in response to the same underlying rainfall data resolved at hourly, daily, and weekly resolutions, as well as to step changes in rainfall delivery, which is expected under a warming atmosphere. We parameterised the model using rainfall, evaporative demand, and soils data from the semi-arid Walnut Gulch Experimental Watershed (WGEW) in SE Arizona, but we present the results as a generalized study of how rainfall resolution and shifts in rainfall intensity may affect dryland soil moisture at different depths. Our results indicate that hourly or better rainfall resolution captures the dynamics of soil moisture in drylands, and that critical information on soil water content, moisture availability to vegetation, actual evapotranspiration, and deep percolation of infiltrated water is lost when soil moisture modelling is driven by rainfall data at coarser temporal resolutions (daily, weekly). We further show that modest changes in rainfall intensity dramatically shift soil water content and the overall water balance. These findings are relevant to the prediction of soil moisture for crop yield forecasts, for adaptation to climate-related risks, and for anticipating the challenges of water scarcity and food insecurity in dryland communities around the globe, where available datasets are of low spatial and temporal resolution.

1 Introduction

In dryland regions of the world, water is inherently scarce, and there are tight relationships between rainfall and soil moisture that have implications for the water balance and specifically for groundwater recharge, agriculture, and natural vegetation. Given the brevity of storms and high potential evapotranspiration, it is challenging to understand the influence of rainfall on soil moisture in drylands, yet this information is critically needed within drought-prone dryland regions, where livelihoods are coupled to the regional expression of climate (Funk et al., 2019;Davenport et al., 2019). There is a disconnect between the spatial and temporal resolution of globally available rainfall data and the local characteristics of precipitation and its translation into soil moisture and water availability to vegetation within dryland regions. Drylands are characterised by low mean annual precipitation totals, but is expressed through rainstorms that are typically intense, short-lived, and spatially restricted (Nicholson, 2011). Dryland regions, which comprise 40 % of total global land mass, are characterised by extremely scarce water resources and limited in situ data on weather and hydrological fluxes (Nicholson, 2011). These regions tend to have sparse precipitation gauge data, so gridded datasets are typically used to understand the relationships between climate variables and soil moisture, even though they may not preserve the inherent intensity characteristics during individual rainstorms, rainfall sequencing, or the time series of the driving evaporative demand. Globally available (gridded) precipitation data are typically resolved at daily, weekly, and monthly temporal resolutions, and all are in common use for understanding historical expressions of climate into the water cycle, yet it is unclear what effect such aggregated timeframes may have on estimates of soil moisture (and the overall water balance) for dryland regions.

Given the strong feedbacks between rainfall intensity and inherent soil properties such as infiltration capacity, it is not clear how well rainfall data resolved at progressively coarser temporal resolutions might affect the prediction of soil moisture. For example, a 30-minute storm with an intensity of 80 mm/h, would yield 40 mm of rainfall in an hour. Assuming a constant infiltration rate of 20 mm/h, half of this rain would infiltrate into the top layer of soil within an hour (and the other half would pond or run off). However, if this rainstorm was the only rain occurrence that day and precipitation was summed over a day, it would yield 40 mm/day or 1.7 mm/h. This bias towards light, constant drizzle becomes even more extreme for weekly data (0.24 mm/h), and it is clearly not reflective of most dryland rainfall. This so-called ‘drizzle effect’ is a problem that limits how well the climate system is represented at the land surface, and it has already been identified as a major challenge in climate modelling (Pendergrass and Hartmann, 2014;Stephens et al., 2010). However, it is less well appreciated how this drizzle effect might manifest within historical gridded precipitation datasets (based on gauge data, remote sensing, and/or reanalysis climate

https://doi.org/10.5194/hess-2021-48
Preprint. Discussion started: 4 February 2021

modelling) and its broader implications for studies of land surface hydrology that use these data. In this paper, we explore how using rainfall data resolved at different temporal resolutions (hourly, daily, weekly) affect estimates of soil moisture and water availability to plants in dryland regions. We also explore how changes to the delivery of rainfall in the future might affect soil moisture. If precipitation during individual events becomes more or less intense (Trenberth, 2011;Trenberth et al., 2017), it could have major implications for soil moisture, especially in dryland regions, but this effect is currently unknown. We suggest that one of the most critical variables required to understand and predict the soil moisture profile in drylands is rainfall temporal resolution, which is often coarser than the inherent expression of rainfall for hydrological processes.

In order to address these issues, we created decadal timeseries of rainfall inputs at three temporal resolutions (hourly, daily, weekly) with the same seasonal and annual rainfall totals, based on high resolution, long-term data from a densely gauged watershed in SE Arizona. We use these synthetic time series to drive Hydrus-1D, a model based on Richards equation for Darcian flow in unsaturated conditions (Šimůnek et al., 2012), and explore model outputs of soil moisture, actual evapotranspiration, and deep percolation of infiltrated water under different scenarios.

2 Methods

2.1 Study Site

Our goal was to evaluate the effects of temporal rainfall resolution on soil moisture that could be used to inform modelling strategies for data-sparse dryland regions. To accomplish this, we needed a data-rich site, where we could reasonably evaluate conversion of rainfall into soil moisture. The study was carried out using data from Walnut Gulch Experimental Watershed (WGEW), a 150 km^2 semi-arid watershed in SE Arizona, as a proxy for a testbed to explore the impact of rainfall inputs on soil moisture (Figure 1). WGEW is a typical semi-arid region with brush and grass cover, an elevation ranging from 1250 to 1585 m, and annual average precipitation of 350 mm (Renard et al., 2008). Within WGEW, we focused on a location in the Kendall grasslands, where there was available rainfall data from a dense network of rainfall gauges (Figure 1) with per minute resolution spanning multiple decades (Goodrich et al., 2008;Renard et al., 2008), soil moisture data from a mesoscale cosmogenic neutron apparatus (details below). This site is a typical hot arid climate region with a Köppen-Geiger BWh climate classification and an aridity index between 0.05 and 0.20. This area is characterised by high evaporative demand and intense convective rainstorms during the summer monsoon, which dominate annual runoff in the basin (Osborn and Lane, 1969;Osborn et al., 1979;Goodrich et al., 2008).

https://doi.org/10.5194/hess-2021-48
Preprint. Discussion started: 4 February 2021

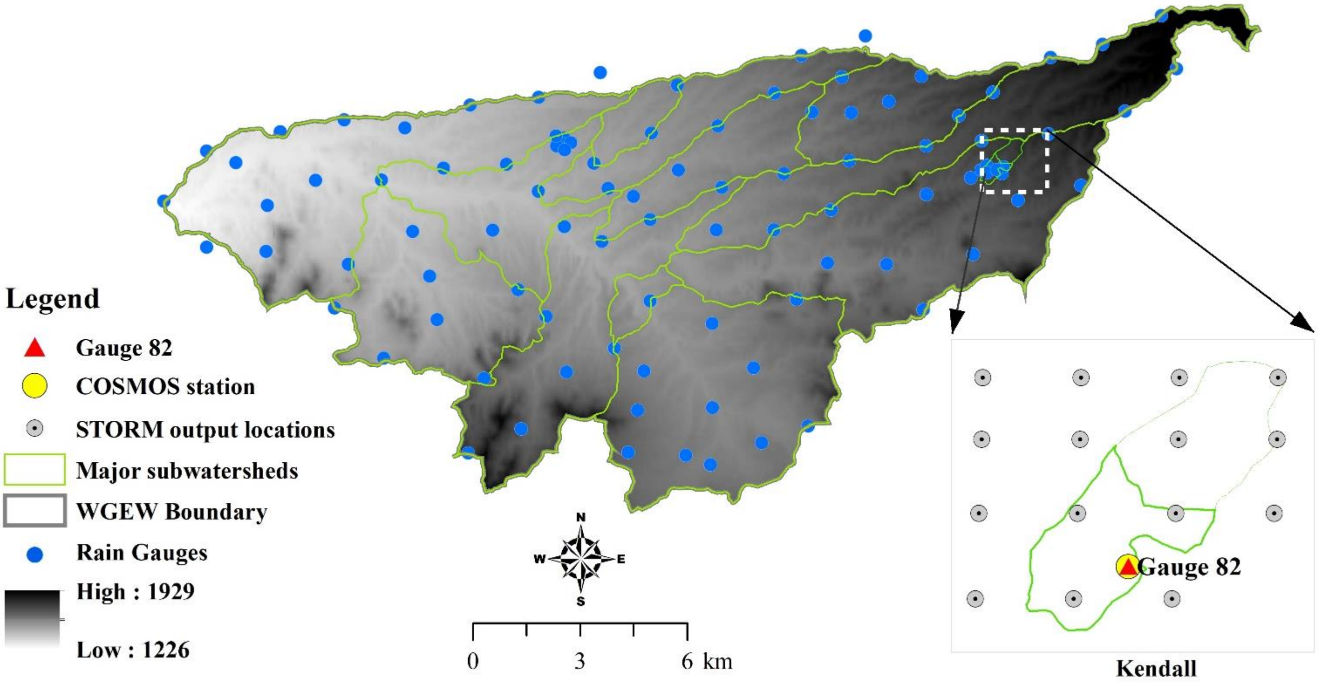

Figure 1. Map of WGEW showing rainfall gauging stations and an insert map that shows location of Kendall station, the mesh of hypothetical rainfall locations around the Kendall site, which were used to develop the climate change scenarios in the STORM model.

2.2 Modelling Strategy

In this study we used the Hydrus-1D model v4.17 (Šimůnek et al., 2012) to simulate soil moisture dynamics in response to different rainfall resolutions (hourly, daily, weekly) over a multi-decadal period (2000-2019). Hydrus-1D has been applied to understand and track water flow through porous media and it has been extensively tested and successfully applied worldwide in many different conditions. The model is driven by time series of rainfall and potential evapotranspiration (PET), from which the water balance is solved numerically to determine net rainfall, infiltration into the upper soil layer, actual evapotranspiration, and drainage below the bottom layer (Figure 2). Hydrus-1D solves the Richards equation, the unsaturated form of Darcy's Law, to quantify movement of water through the soil, between soil and the atmosphere (via evapotranspiration), and the percolation of soil water into the groundwater aquifer. The model requires parameterisation of soil properties that control water flow through the soil (e.g., hydraulic conductivity), which can be derived from soil texture (van Genuchten, 1980). Details on the model development and theoretical underpinning can be found elsewhere (Šimůnek et al., 2012).

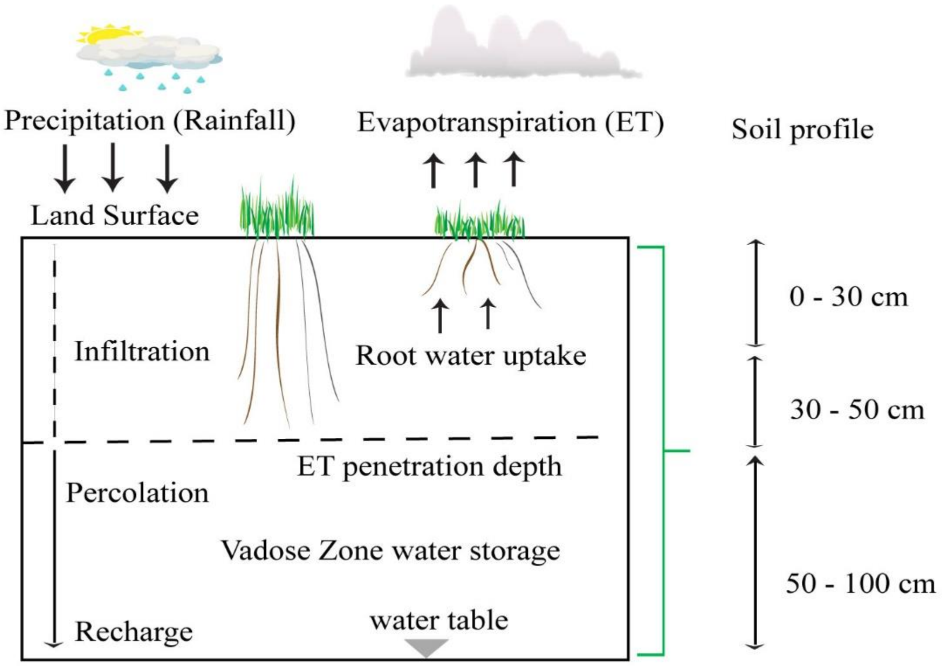

Figure 2: (a) Conceptual figure for water partitioning at the soil vadose zone (b) Discretisation of soil moisture content at three depth intervals in the soil profile: 0-30, 30-50 and 50-100 cm.

2.3 Input Data

We used the data-rich WGEW as a representative testbed for understanding the impacts of rainfall resolution and rainfall intensity on soil moisture in dryland regions. Event precipitation data were acquired from rainfall digital gauging station (No. 82) within WGEW (Figure 1; www.tucson.ars.ag.gov/dap/). This site lies near the Kendall Grasslands where soil moisture has been monitored by two methods, enabling evaluation of our modelling. On site, there is a COsmic-ray Soil MOisture Sensor (COSMOS) station (31.7368N, -109.9418E) operating since 2010 (http://cosmos.hwr.arizona.edu/Probes/StationDat/010/index.php), which measures soil moisture at a radius of order ~10^2 m and to depths of order ~10^{-1} m using cosmogenic neutrons. COSMOS is a mesoscale measure of soil moisture based on an area and depth averaging. Soil moisture from cosmic-ray neutron sensors from Kendall site was obtained directly from the COsmic-ray Soil Moisture Observing System (COSMOS) (Zreda et al., 2012). Typical corrections to measured neutron counts related to variations of atmospheric pressure and water vapor, and solar intensity were applied following guidelines in the literature (e.g., (Rosolem et al., 2013;Schrön et al., 2017)). In addition, the cosmic-ray neutron sensor at Kendall was calibrated against independent set of soil samples taken within the sensor footprint as part of its original deployment and all information is available in the COSMOS network (e.g., dry soil bulk density, soil lattice water, soil organic carbon, and sensor calibration coefficient N0). Additional data quality control steps were taken by removing unrealistic estimates of soil moisture by the cosmic-ray neutron sensor that fell either below zero volumetric (m^3 m^{-3}) soil moisture content or above the site-specific porosity of 0.54 cm^3 cm^{-3}. Finally, a 12-hour moving average was applied to smooth the time-series as commonly done at other COSMOS network sites (Zreda et al., 2012).

To obtain rainfall intensity per event from the historical WGEW rainfall record, we divided reported event precipitation depth (mm) by event duration (min), and then aggregated the resulting set of events into hourly precipitation data (Figure 3). We subsequently aggregated this synthetic hourly time series of precipitation into daily and weekly series, ensuring that the total rainfall volume is the same in each time series (Figure 4). The temporal spreading of rainfall data from hours to weeks has a very noticeable impact on the mean values of precipitation (Figures 4a-4c) and on the peak magnitudes of events (Figures 4d-4f). Although the WGEW rainfall record goes back to the 1950s, we modelled precipitation inputs from the year 2000, in order to ensure that the input rainfall series coincide with the available reference crop evapotranspiration (ET_O) data (a measure of potential evapotranspiration).

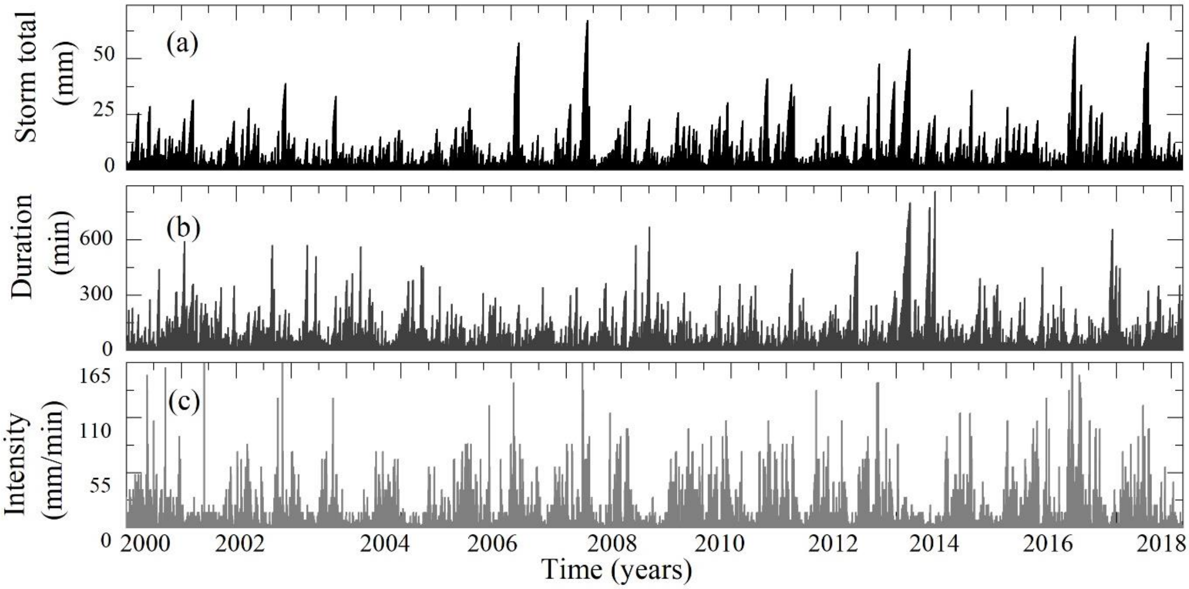

Figure 3: Storm event totals, durations, and calculated intensities for rainfall at digital gauging station #82 in WGEW, Arizona, USA over the period 2000-2019.

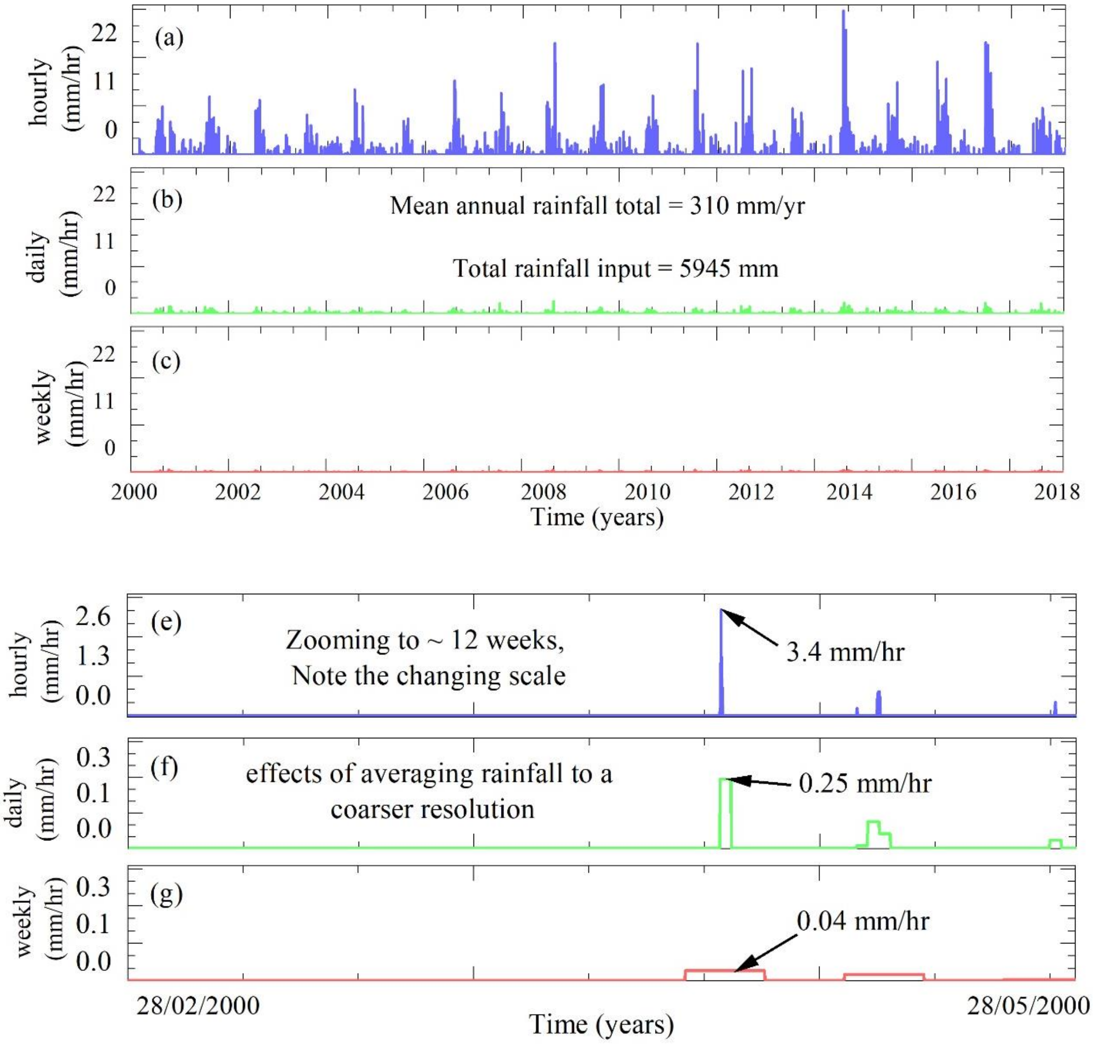

Figure 4: Rainfall timeseries used to drive Hydrus-1D obtained from rain gauge data at WGEW for the period 2000-19. Plots show a) hourly, b) daily and c) weekly resolutions derived from the original data. The mean annual rainfall (330mm/yr) and total rainfall input over the two decades are shown (5945 mm). Panels e, f and g are zoomed in for the 3-month period beginning 28/02/2000.

In order to characterise atmospheric evaporative demand, we downloaded a time series of reference crop evapotranspiration (ET_O) at hourly resolution (Figure 5) from a weather station at Tucson, Arizona (https://cals.arizona.edu/AZMET/01.htm). The station is part of the Arizona Meteorological Network (AZMET) and is located at 32.280248N, -110.938718E, approximately 60 miles from WGEW at an elevation of 717 m, which we assume would experience similar evaporative demand to the Kendall site at WGEW. The AZMET ET_O is calculated based on modified form of Penman-Monteith Equation (Eq. 1), which is representative of evaporative demand in the atmosphere (Brown, 2010):

$$ET_O = \frac{0.408\Delta R_n + \gamma \frac{900}{T+273} u_2 (e_s - e_a)}{\Delta + \gamma(1 + 0.34u_2)} \qquad (1)$$

where Δ is the slope of the saturation vapor pressure-temperature (kPa $^{\circ}$C^{-1}), R_n is net radiation calculated at the crop surface in MJ m^{-2} h^{-1}, γ is psychrometer constant (kPa $^{\circ}$C^{-1}), u_2 is average hourly wind speed measured at 2 m above ground level (m s^{-1}), T, is average air temperature at 1.5 m above ground level ($^{\circ}$C), e_a and e_s are saturation vapor pressure and mean actual vapor pressure respectively all measured at 1.5 m from the ground level (kPa).

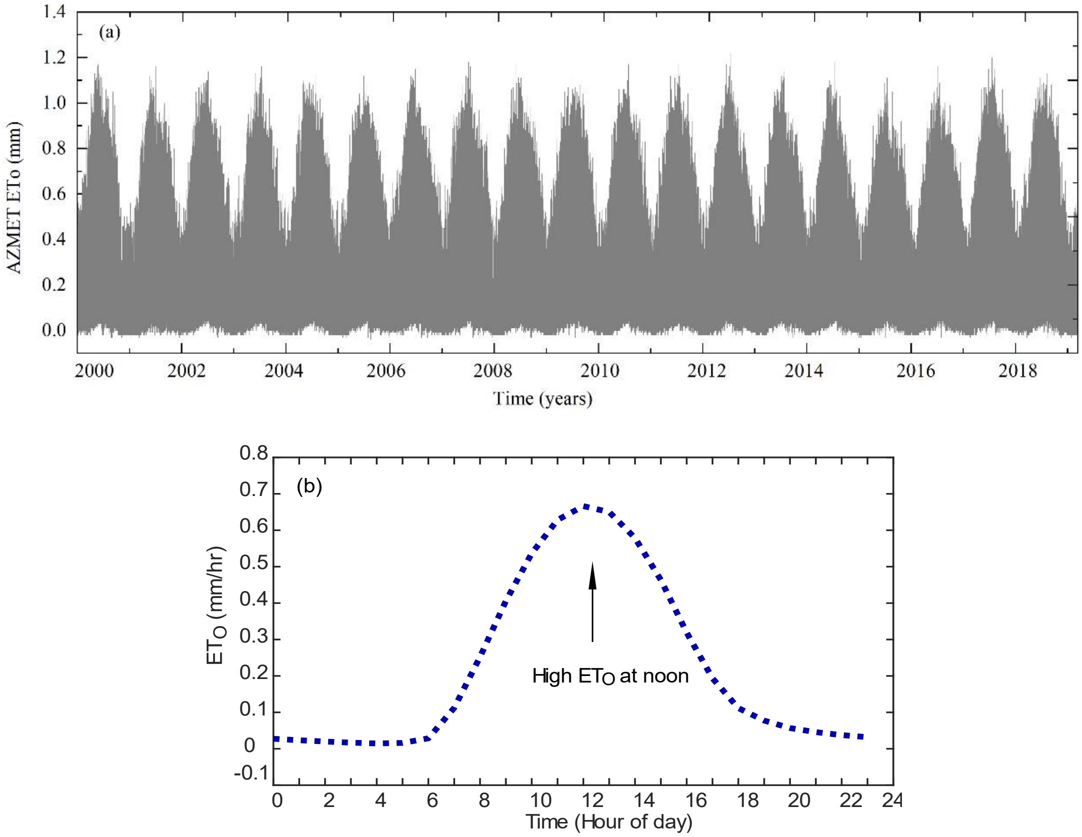

Figure 5: (a) Distribution of hourly reference crop evapotranspiration (ET_O) for the time 2000-2019 obtained from AZMET, computed by Eq. (1), showing the seasonal cycle and (b) the characteristic diurnal cycle of evaporative demand for a day.

2.4 Modelling Soil Moisture

Hydrus 1-D requires separate values of both potential evaporation (E_p), the upper boundary, and potential transpiration (T_P), represented within the sink term in Richards equation. Beer's law was used to partition AZMET ET_O to (E_p) and (T_P) based on the Leaf Area Index (*LAI*) (Ritchie, 1972):

$$T_p = ET_O\left(1 - e^{-k^*LAI}\right) \qquad (2)$$

$$E_P = ET_O e^{(-k*LAI)} \qquad (3)$$

where k represents the extension coefficient for solar radiation at global scale, and is a function of angle of the sun, leaf arrangement and distribution of plants. Here we adopted k of 0.463, as in previous work (Tuttle and Salvucci, 2016;Šimůnek et al., 2012;Chen et al., 2014). The partitioned hourly ET_O values were used as model input to compute the water balance and were kept constant over all simulations, regardless of the timescale or intensity of the input precipitation. The model is spatially discretised in 1cm layers and we integrate soil moisture outputs over 0-30 cm, 30-50 cm and 50-100 cm. At the bottom of the soil, we used a free drainage water flow boundary (zero-gradient) condition to simulate a freely draining soil profile, assuming the water table is deep enough to not influence water redistributions in the soil profile. Hydrus-1D provides various relevant water balance outputs including soil moisture at multiple depths through the soil profile, actual evapotranspiration, and free drainage, which gives information on deep percolation of infiltrated rainfall that will likely contribute to groundwater recharge.

Rainfall gauging station number 82 at WGEW lies in the Elgin-stronghold soil complex (https://www.tucson.ars.ag.gov/dap/1993soils.htm). By averaging 9 data points covering the whole Elgin-stronghold soil complex within the Kendall, we obtained averaged soil texture of ~79 % sand, ~11 % silt, and ~9 % clay (Breckenfeld et al., 1993). We used the neutral network prediction module in Hydrus-1D, based on the Rosetta model (Schaap et al., 2001), to determine soil water retention and suction parameters required to compute soil moisture. To parameterise saturated hydraulic conductivity (K_s), we used published data from rainfall simulation experiments in WGEW (Wainwright et al., 2000). The soil for the Kendall site is represented in Hydrus-1D as a uniform soil profile with parameters shown in Table 1.

Table 1: Hydrus-1D modelling parameters and value ranges used in this study based on measured soil texture and grassland vegetation for WGEW.

	Parameter	Value	Unit	Source/calculation method
	Meteorological parameters to calculate PET			AZMET data set (https://cals.arizona.edu/AZMET/)
P	Hourly precipitation			WGEW (https://www.tucson.ars.ag.gov/dap/)
	Soil hydraulic parameters			
θr	Residual soil water content	0.04* or θ_s 7.4 %		Calculated using Rosetta (Schaap et al., 2001)
θ_{SAT}	Saturated soil water content	0.5364* or θ_s 100 %		Estimated from soil properties at WGEW
K_s	Saturated hydraulic conductivity	5.8020	cm h^{-1}	(Wainwright et al., 2000)
L	Tortuosity parameter in the conductivity function	0.5000		(van Genuchten, 1980)

α	Van Genuchten parameter related to air entry suction	0.0356		Calculated using Rosetta (Schaap et al., 2001)
n	Van Genuchten parameter related to pore size distribution	0.0500		Calculated using Rosetta (Schaap et al., 2001)
	Vegetation parameter			
D_r	Rooting depth	0-30	cm	(Breckenfeld et al., 1993)
D_s	Depth of soil	0-100	cm	(Breckenfeld et al., 1993)
$P0$	Value of the pressure head below which roots start to extract water from the soil.	−1	cm	Hydrus-1D internal database (grass)
$P0_{pt}$	Value of the pressure head below which roots extract water at the maximum possible rate	−20	cm	Hydrus-1D internal database (grass)
P_{2H}	Value of the limiting pressure head, below which roots cannot longer extract water at the maximum rate (assuming a potential transpiration rate of r2H).	−300	cm	Hydrus-1D internal database (grass)
P_{2L}	Value of the limiting pressure head, below which roots cannot longer extract water at the maximum rate (assuming a potential transpiration rate of *r2L*).	−1 000	cm	Hydrus-1D internal database (grass)
$P3$	Feddes parameter	−1 600	cm	Hydrus-1D internal database (grass)
$r2H$	Potential transpiration rate-upper bound (Feddes parameter for grassland)	0.020	cm h^{-1}	Hydrus-1D internal database (grass)
$r2L$	Potential transpiration rate-lower bound (Feddes parameter for grassland)	0.004	cm h^{-1}	Hydrus-1D internal database (grass)
α_i	Interception constant	1	cm	Hydrus-1D internal database (grass)

2.5 Climate Change Scenarios

In order to examine the potential effects of climate change on rainfall and soil moisture in a dryland region, we utilised the STOchastic Rainfall Model (STORM 1.0) developed to generate rainfall time series based on simplified climate change assumptions (Singer and Michaelides, 2017;Singer et al., 2018). STORM 1.0 employs an empirical stochastic approach for rainstorm simulation that allows statistical characterisation of rainfall over a high-resolution grid within a drainage basin and allows for simulation of climate change scenarios. Specifically, we produced rainfall time series for three scenarios under a stationary climate (no change in seasonal or annual wetness): 1) the 'historical' climate scenario based on 20 years of rain gauge data at hourly resolution from the years 2000-2019 at WGEW; 2) an 'increased storminess' scenario based on a 25 % increase in rainfall intensities of all rainstorms relative to the historical period; and 3) 'decreased storminess' based on 25 % decrease in rainfall intensities of all rainstorms relative to the historical period. In this region of the world, rainfall intensities declined significantly over several decades prior to the year 2000 (Singer and Michaelides, 2017;Pascale et al., 2017), but they have been increasing in recent decades with a presumed intensification of the summer monsoon (Luong et al., 2017), warranting exploration of the impact of both scenarios. To accomplish this, we used an ensemble average from 15 rainfall grid locations (Figure 1), covering an area of WGEW where soil moisture has been well monitored. To ensure that our simulations

https://doi.org/10.5194/hess-2021-48
Preprint. Discussion started: 4 February 2021

were robust, we produced 10 realisations for each grid location per climate scenario, equivalent to 200 years of simulation time per scenario.

3 Results

3.1 Model evaluation

Simulated soil moisture saturation (θ_s) values in units of percent were compared with θ_s from COSMOS over the period 2010-2014 (Figure 6). In general, we found good agreement between modelled and observed θ_s and the simulated and observed distributions. Although the distributions are statistically different based on the Kolmogorov-Smirnov statistic ($p< 2.2e-16$), due to the larger range of the COSMOS data (Figure 6), the Mann-Whitney U test showed the medians of COSMOS and Hydrus-1D output are statistically similar ($p=0.5774$). It is clear that the Kendall soil is very dry with a median value of ~18 % saturation, but there are clearly short-lived wet periods wherein high rainfall produces spikes in soil moisture (represented as outliers in both simulated and observed distributions of θ_s in Figure 6). From this analysis, we concluded that Hydrus-1D simulations are broadly representative of measured soil moisture at our study site, enabling further investigation of the effects of temporal rainfall distribution and intensity.

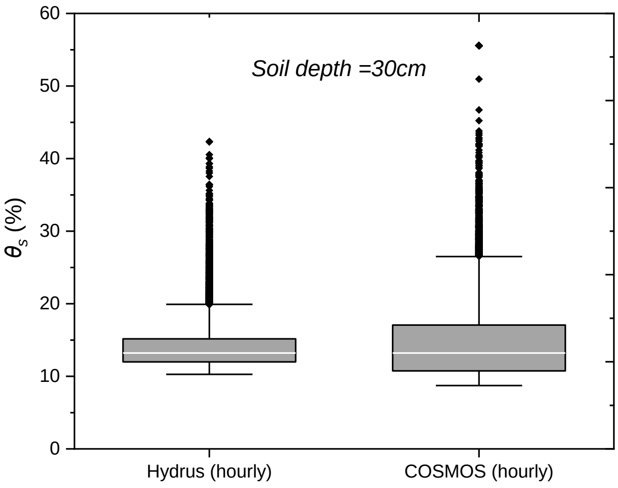

Figure 6: Comparison of hourly modelled (Hydrus-1D) soil moisture versus *in situ* measured soil moisture obtained from COSMOS.

3.2 Effects of rainfall temporal resolution on soil moisture

We investigated the impact of changing rainfall resolution in terms of the overall distribution of rainfall inputs over multiple decades. Based on statistical analysis via the Kolmogorov-Smirnov test, we found highly significant differences between hourly v. daily, hourly v. weekly, and daily v. weekly rainfall (Figure 4; p<<2.2e-16). This suggests that deriving rainfall from gridded data products resolved at different temporal scales can dramatically affect the input time series of rainfall, even if the overall seasonal and annual precipitation totals are the same.

We subsequently analysed the impacts of temporal averaging hourly precipitation over coarser timescales on the resulting soil moisture. The output histograms of θ_s for the three input rainfall resolutions (hourly, daily, weekly) and for the three depth intervals are shown in Figure 7. They illustrate that strong differences in the temporal expression of rainfall have a large impact on the resulting soil moisture for all depth intervals. At each soil profile layer, the soil moisture values produced by the three rainfall resolutions are highly significantly different from each other (p<2.2e-16) for both comparisons of distributions (Kolmogorov-Smirnov) and their medians (Mann-Whitney), where the median declines with increasing time interval of rainfall aggregation.

Another interesting aspect of these plots is how shifts in soil moisture distributions arising from different temporal resolutions of input rainfall affect the time below wilting point (WP), which has important implications for plant (and crop) water availability. The frequency of values that cross below the WP threshold progressively increases (lower soil moisture) with increasing temporal resolution of rainfall, moving from hourly to weekly (Figure 7a-c). These are important results, which were anticipated based on the marked differences between distributions of input rainfall (Figure 4). They indicate the ‘drizzle effect’ in which temporal aggregation leads to a steady supply of precipitation to the land surface at very low intensity, is counteracted by actual evapotranspiration losses for the upper 30 cm of soil, leading to a drier soil column (Figure 7a). This phenomenon underlines the importance of resolving rainfall at the appropriate temporal scale to characterise the infiltration and resulting soil moisture and water availability to relevant vegetation at different rooting depths. Remarkably, the weekly and daily input rainfall distributions yield soil moisture values for the upper 30 cm of soil that are below the WP 7-8 % more of the time than moisture values from hourly rainfall. In other words, the results indicate substantially different conditions for plant (crop) water stress, depending solely on rainfall resolution. Even for the 30-50 cm depth interval, the weekly rainfall resolution results in soil moisture below the wilting point 59 % of the time over the 20-year simulation, due to losses in the upper layer and a lack of development of a strong wetting front under prevalent drizzle conditions.

https://doi.org/10.5194/hess-2021-48
Preprint. Discussion started: 4 February 2021

260

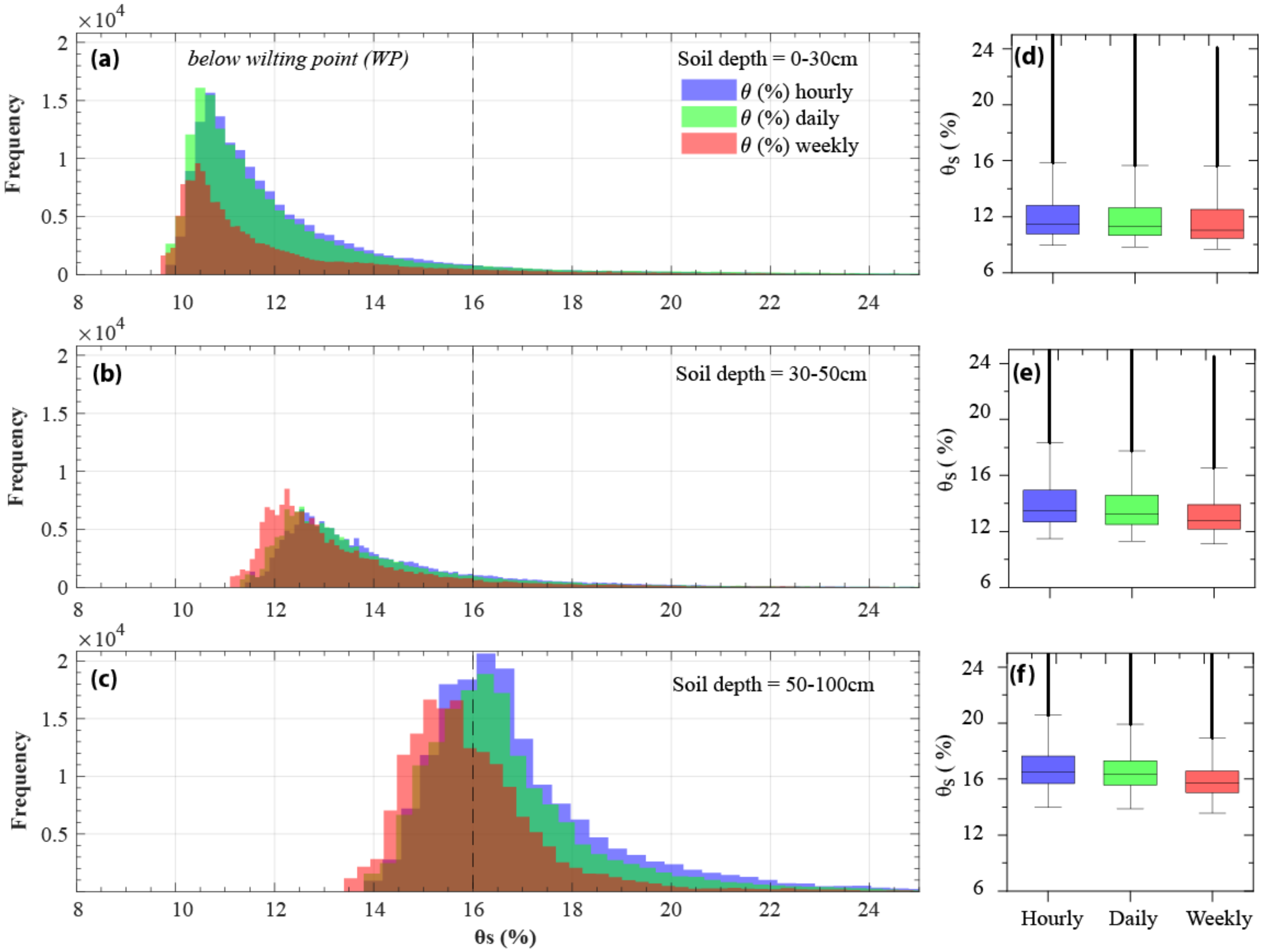

265

Figure 7: Modelled soil moisture distributions for the three rainfall resolutions (hourly, daily, weekly) over decadal timeseries simulations at (a) 0-30 cm, (b) 30-50 cm, and (c) at 50-100 cm layer of the soil profile, and the corresponding distributions as boxplots (d-f). The dashed lines in a-c denote the wilting point (WP).

The amount of *P* lost via AET decreases as we move from weekly to hourly rainfall resolutions (Figure 10). For example, over 270 the period 2000-2019 at WGEW, hourly precipitation produced cumulative AET of 3720 mm, while the daily simulation generated ~10 % more AET, followed by the weekly simulation with 28% more AET (Fig.10). The deep percolation below the model domain decreased with reduced rainfall resolution from the hourly cumulative value of 2146 mm to ~18 % less for daily rainfall, and 49 % less for weekly rainfall Out of the cumulative *P* of 5945 mm that enters the water balance, AET tends to be more than double the value of drainage for all the three resolutions (Fig.10).

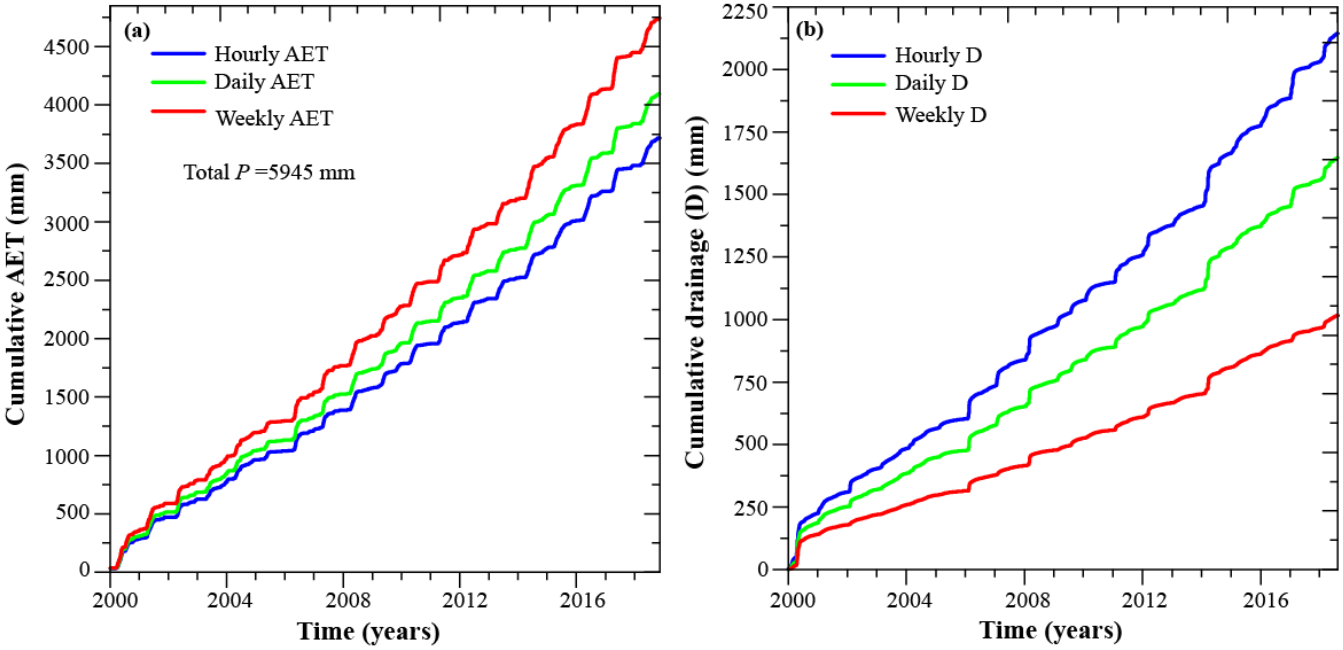

275

Figure 8: Cumulative AET (a) and cumulative drainage (b) produced by modelling the three rainfall resolutions. The cumulative *P* for all the three resolutions is 5945 mm. The AET for hourly, daily, and weekly resolutions when expressed as a percentage of total precipitation is respectively is 62 %, 69 % and 80 % while the percentages for drainage when expressed as percentage of P is 36 %, 30 % and 18 %, respectively.

280 3.2 Climate change scenarios and rainfall characteristics

Based on the understanding gained from changing input rainfall resolution, we further explored the impact of hypothetical scenarios of climate change on soil moisture using only hourly timeseries of rainfall, since this temporal resolution well captures the influence of dryland rainfall characteristics on soil moisture (Figure 6). The two climate scenarios investigated here (increased and decreased rainfall intensity with no change to seasonal or annual precipitation totals) are distinct from the 285 'historical' baseline timeseries generated stochastically from rain-gauge data in WGEW over the 20-year simulation period (Figure 8). Rainfall intensities, in terms of both distributions (Kolmogorov-Smirnov) and medians (Mann-Whitney), are significantly different between the three climate scenarios ($p<2.23e-308$), for example, where the 'decreased storminess' scenario produces more storms (at lower intensity) and the 'increased storminess' scenario produces fewer, but more intense storms relative to the 'historical' baseline timeseries (Figure 8).

290

Table 2: Kolmogorov-Smirnov (KS) and Mann-Whitney (U) tests for comparison of changes in storm intensities under the three climate change scenarios

	KS-test	KS p-value	U-Statistic	U p-value

'Historical' climate vs 'decreased storminess'	0.0053	2.3314e-20	9.0461	1.4823e-19
'Historical' climate vs 'increased storminess'	0.0032	8.4973e-08	-11.9744	4.8405e-33
'Increased storminess' vs 'decreased storminess'	0.0084	9.4712e-55	21.9586	7.1635e-107

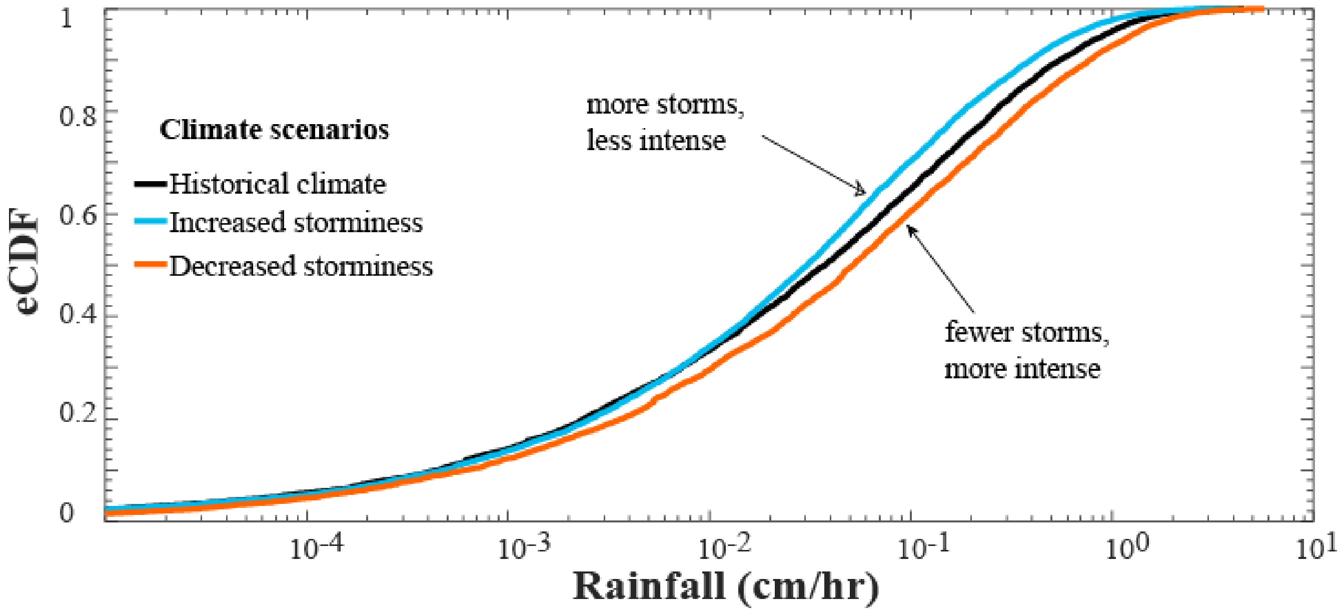

Figure 9: Empirical cumulative distribution functions (eCDFs) of 'historical' (black), 'decreased storminess' (yellow) and 'increased storminess' (red) climate scenarios precipitation intensities.

The hourly rainfall timeseries for the baseline (historical) and the two climate change scenarios were used to examine the relative impacts of these differences in overall rainfall intensity characteristics on soil moisture dynamics using Hydrus-1D. The modelled soil moistures using the three climate scenarios were all significantly distinct from one another (Table 2). Relative to the historic 'baseline' conditions, the distribution of soil moisture produced by the 'decreased storminess' scenario is generally lower (skewed to the left) for all soil depth intervals, while it is higher (skewed to the right) for the 'increased storminess' scenario (Figure 10). The differences between the distributions become larger with soil depth. For example, the differences in time below the wilting point between the 'decreased storminess' simulation and the other two simulations increases sharply in the 30-50 cm interval, and again for the 50-100 cm interval. It is clear that the 'historical climate' and 'increased storminess' simulations generate significant wetting fronts that persist at deeper soil depths, such that there is a minority of the distribution below the wilting point (Figs 10a and 10b). Additionally, we detected a crossover between the ‘historical climate’ and ‘increased storminess’ scenarios in the 50-100 cm depth interval, whereby the historical distribution of θ_s exceeds that of the decreased storminess up to the 15th percentile, above which the ‘increased storminess’ distribution of θ_s for the higher intensity rainstorms yields an overall wetter soil (Figure 10).

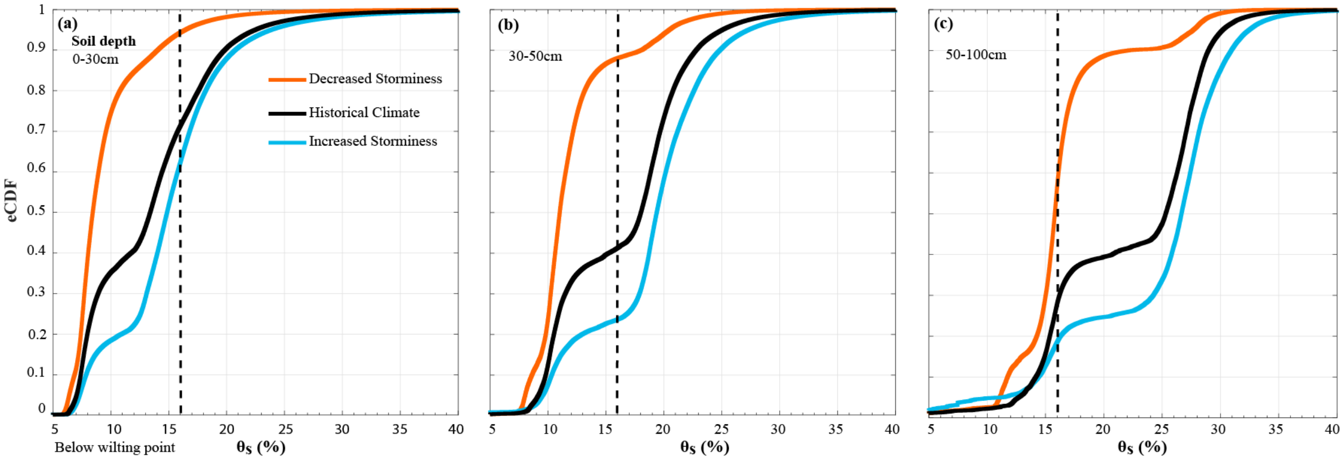

Figure 10. Empirical cumulative distribution functions (eCDF) of modelled θ_s produced by the three climate scenarios at (a) 0-30 cm, (b) 30-50 cm, and (c) 50-100 cm. The top 0-30 cm of the soil profile is below WP 71 %, 94 % and 62 % of the time, respectively for historical, decreased storminess, and increased storminess, respectively. At the 30-50 cm soil depth, θ_s was below WP 41 %, 88 % and 23 % of the time for historical, decreased storminess, and increased storminess, respectively. The bottom 50-100 cm interval of the soil had θ_s values WP 30 %, 56% and 18 % for historical, decreased storminess, and increased storminess respectively during the whole simulated period.

Partitioning of precipitation into AET and deep percolation (drainage below the model boundary) for these climate change scenarios supports the expectation of lower (higher) cumulative loss of water through evapotranspiration for increased (decreased) storminess. Essentially less intense rainfall infiltrating into upper soil layer tends to be lost more easily than intense rainfall that penetrates deeper in the profile through a pronounced wetting front. Consequently, the results show more water draining below the bottom of the soil profile in the ‘increased storminess’ scenario than in the other two. Note that the use of stochastic ensembles of rainfall results in more variability in these results and perhaps more overlap than might otherwise be expected.

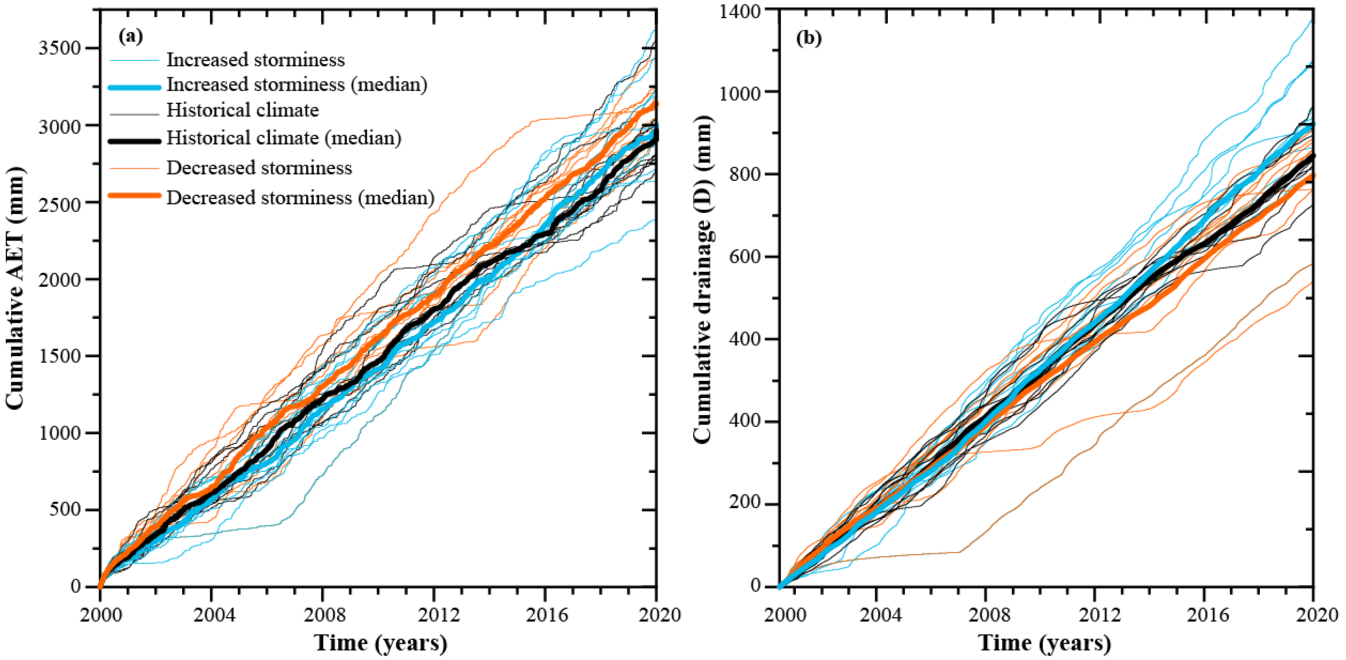

Figure 11. Cumulative AET produced by the three climate scenarios (a), (b) is the cumulative drainage. At the end of 20 years of simulation, cumulative AET is 3138 mm, 2964 mm and 3003 mm for reduced storminess, historical climate, and increased storminess scenarios respectively while the cumulative drainage is 1247 mm, 129 3mm and 1376 mm for reduced storminess, historical climate, and increased storminess scenarios, respectively.

4 Discussion

Drylands are water-limited environments facing immense challenges under climate change. In the most food insecure dryland regions of the world, the lack of ground-based meteorological stations increases the uncertainty in forecasting soil moisture and crop yields over seasonal time horizons, and also in the projection of changes to the water balance under climate change. As a substitution for local precipitation information, data from individual meteorological stations is often gridded, sometimes using remote sensing data and/or global climate model reanalysis data, to obtain spatially consistent characterisations of rainfall (and ET) to quantify the water balance and thereby determine plant-available water and associated crop yields. These calculations then typically form the basis for decision support tools and famine forecasts (Funk et al., 2019;Brown et al., 2017). Given that most gridded rainfall products generated in this manner are available on daily or coarser temporal resolutions (e.g., daily data for Global Precipitation Climatology Centre-GPCC and 5-day averages for CHIRPS (Funk et al., 2015)), we explored how these temporal resolutions affect estimates of soil moisture, especially in drylands where rainfall is often delivered in brief rainstorms that are challenging to represent in climate and hydrological models (Nicholson, 2011;Singer et al., 2018). For example, rainstorms often occur on timescales of hours and even portions of hours, delivering water to the land surface at high intensity, where it infiltrates into dry soils on flat ground at high rates.

Through our 1D modelling, we found systematically lower soil moisture distributions for progressively coarser temporal resolutions of input rainfall (Figure 7), despite the same total precipitation. This phenomenon arises due to nonlinear interactions between the rainfall resolution and the Richards equation (Wang et al., 2009), and corresponding subsurface propagation of the 'drizzle effect', a term usually restricted to climate modelling, but here used to refer to the effect of temporally averaging precipitation. If a single intense rainstorm of 100 mm/h lasting for 50 minutes is averaged over a day or a week, it will yield a constant input of very light rainfall (Figure 4), which may be easily counterbalanced by AET losses over a diurnal cycle (Figure 5). Further exploration of the effect of rainfall resolution on soil moisture showed that the differences between hourly input rainfall versus daily and weekly values becomes more pronounced with depth in the soil, as the effects of rainfall resolution propagate through the wetting front. In particular, the coarser temporal resolutions lead to higher AET losses of infiltrated precipitation (Figure 8), lower soil moisture with more time below the wilting point at deeper depths (Figure 7), and less deep percolation (Figure 8), which might support more deeply rooting plants and crops, or recharge groundwater aquifers via diffuse recharge. If one were to propagate these soil moisture values into crop yields for these shallow rooting depths, they would dramatically underestimate the water availability to critical crops and therefore underestimate crop yields and overestimate the risk of crop failure and corresponding famine for many years of the historical time series. Our results also indicate that moving from hourly to daily to weekly rainfall resolutions in hydrological modelling may lead to 16 % and 45 % underestimation of groundwater recharge (deep percolation), respectively. This result of higher moisture availability at deeper depths could have important implications for more deeply rooted forage crops and native vegetation that serves as a critical food source to livestock in pastoralist communities in dryland regions around the world.

When seasonal rains fail in dryland regions that rely on rainfed subsistent agriculture and pastoralism, it threatens livelihoods and often requires large-scale humanitarian response from governments and NGOs to avert famine. The rural communities within the Horn of Africa drylands (HAD) are particularly prone to climatic shocks and they tend to have low socio-economic levels, and low adaptive capacity to climatic shocks. Hence, recent severe droughts have dramatically increased food insecurity from ~7 million people in 2011 to ~35 million people in 2017, leading to livestock loss and major water shortages. The region has a total population of 160 million people, 70 million of that population live in areas classified as having extreme food shortage, other 40 % of the population is undernourished (Lusamba-Dikassa et al., 2012;Margulis, 2012). Over the last four decades, droughts in HAD have become more frequent and more severe (Lyon and DeWitt, 2012;Liebmann et al., 2014;Funk et al., 2019), reducing soil moisture for plants and affecting groundwater reserves. Therefore, there is increasing need to improve characterisation of drought (and flood) impacts on water stores such as soil moisture (Gruber et al., 2019). Current analyses of soil moisture are often based solely on remote sensing data, which only provides information on the top ~5-10 cm of the soil profile. Other work calculates soil moisture and crop yields based on globally available precipitation data at daily or weekly resolutions (Harrison et al., 2019). Our analysis suggests that in dryland regions, where precipitation is often delivered in brief, intense storms, it is important to model the impacts of rainfall forecasts on water storage using precipitation data at high temporal resolution, in order to more faithfully capture its effects. Indeed our results from 1D modelling (Figure

8) corroborate the results form previous work suggesting that rainfall intensity is closely linked with groundwater recharge (Adloff et al., In Review;Taylor et al., 2013;Cuthbert et al., 2019).

To overcome the challenges of representing projections of precipitation in dryland regions and its impact on soil moisture, where evaporative demand is extremely high, we opted to investigate climate change using bespoke scenarios that simply modify the rainfall intensity for individual storms (termed ‘storminess’ here) by ±25 %, while maintaining the same seasonal distribution of total rainfall (Singer et al., 2018). This approach, consistent with previous observations that changes in rainfall intensity may arise within higher resolution rainfall data (Barbero et al., 2017;Guerreiro et al., 2018), enables characterization of the impact such intensity changes may have on the water balance for a region. An ensemble of multiple stochastic simulations done in this manner provide a more robust picture of the likely impact that changes in rainfall intensity will have on soil moisture, AET, and deep percolation. Specifically, we found that systematic differences between inputs (stochastic simulations of stationary historical rainfall, of increased storminess, and decreased storminess (Figure 9) lead to markedly different soil moisture distributions (Figure 10), as well as in notable differences in AET and drainage below the bottom boundary (Figure 11). The differences in soil moisture between simulations become larger with depth, as higher intensity rainfall is characterized by deeper wetting fronts that promote longer retention of infiltrated moisture. Figure 12 sheds more light on this effect for a series of rainfall events over the years 2008 and 2009, where the penetration depth of individual rainfall events declines from hourly to daily to weekly rainfall resolutions (black arrow shows same rainfall event in each series). It is also apparent from these soil moisture profiles in time series that higher rainfall intensity leads to higher overall moisture content at deeper depths (more yellow colouring in Figure 12), and also likely contributes to groundwater recharge.

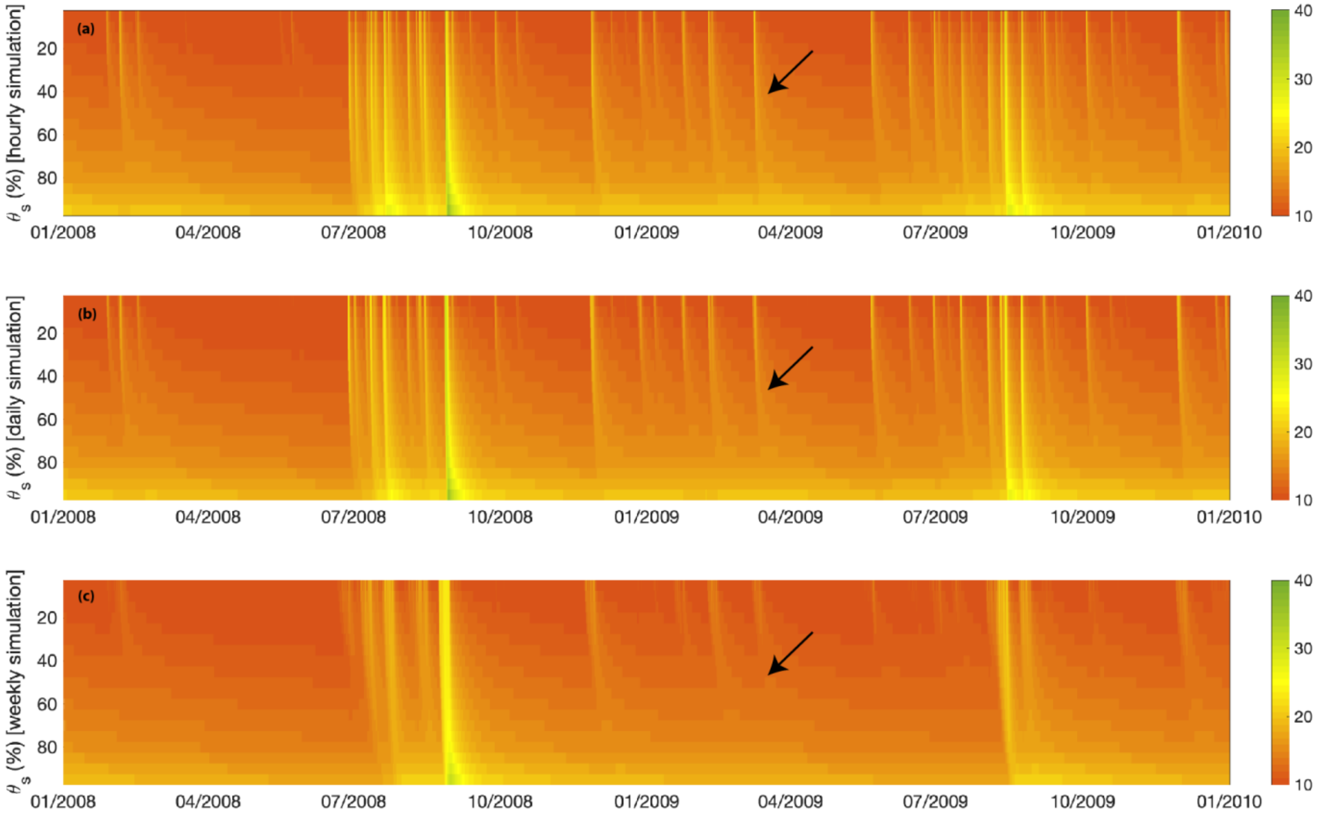

Figure 12. Soil moisture profile for hourly, daily, and weekly series showing a strong wetting front at the end of monsoon seasons of the years 01/01/2008-30/12/2009. Arrows show differences in the penetration depth of soil moisture for the same rainfall event for the three temporal resolutions.

These seemingly small differences could have a major influence on water availability to vegetation in dryland regions, and thus rural livelihoods in subsistence regions like HAD. In summary, if rainfall in regions such as HAD becomes more intense due to atmospheric warming, it may support more higher soil moisture and higher groundwater recharge, therefore supporting more sustainable rainfed agriculture, pastoralism, and human drinking water supplies from wells. However, under historical climate or the decreased storminess climate scenario (at least based on the data for Walnut Gulch), the landscape would remain dry for much of the year, creating challenging conditions to raise crops or grow hydrophilic fodder crops.

These results suggest great care should be taken in hydrological modelling to represent input rainfall at the most appropriate temporal (and spatial) resolution to best represent the relevant hydrological processes that affect key water balance components: infiltration, evapotranspiration, and runoff. If rainstorms occur at subhourly timescales, it is not sensible to use daily or weekly rainfall to drive such a model. Instead, we recommend the use of the highest rainfall resolution available (often 15-min for many gauging locations). If there are severe limits to the availability of such data, stochastic models that resolve rainfall at such scales is recommended to drive models of hydrological partitioning (Singer et al., 2018). And given the large uncertainties in projecting future changes in precipitation from global climate models, it is further recommended to explore a range of methods for simulating future rainfall scenarios with trends that seem plausible or which are based on physical concepts. Ultimately, to make progress in forecasting and predicting the effects of rainfall changes to soil moisture (and by extension, runoff, and groundwater recharge) and the cascading impacts to vegetation and human society.

5 Conclusions

In this study we evaluated the impacts of rainfall data resolution as well as impacts of climate change on water partitioning upon reaching the soil surface in dryland environment. We used the Hydrus-1D model, driven by historical and stochastic inputs, and applied it to estimate the soil moisture profile at the Kendall site of WGEW. There we demonstrated the importance of high-resolution rainfall data in best characterising the soil moisture and time below wilting point and explored the potential effects of shifts in rainfall intensity associated with climate change. We discussed the broader implications for subsistence communities living in drylands globally. Our straightforward modelling approach yielded new insight into the links between the climate system and soil moisture storage and the water balance in drylands.

Competing interests. The authors declare no conflict of interest.

Author's Contribution. IK, KM, RR and MBS designed this study. IK performed the model Simulations MBS and KM provided the model data for the climate change simulations. KM, RR and MBS assisted IK in result analysis and discussions. All authors contributed to writing and revising the manuscript.

Acknowledgements. This work was supported by grants from the US National Science Foundation (BCS-1660490 and EAR-1700555) and the US Department of Defense's Strategic Environmental Research and Development Program (RC18-1006) to MBS. We also acknowledge support to KM from Global Challenges Research Fund (GCRF) grant 'Impacts of Climate Change on the Water Balance in East African Drylands', The Royal Society (Grant CHL\R1\180485), and the European Union's Horizon2020 (Grant 869550).

References

Adloff, M., Singer, M. B., MacLeod, D., Michaelides, K., Mehrnegar, N., Hansford, E., Funk, C., and Mitchell, D.: Groundwater storage in East African drylands dominated by increasing intensity of seasonal rainfall, In Review.

Barbero, R., Fowler, H. J., Lenderink, G., and Blenkinsop, S.: Is the intensification of precipitation extremes with global warming better detected at hourly than daily resolutions?, Geophys. Res. Lett., 44, 974-983, 10.1002/2016gl071917, 2017.

Breckenfeld, D., Svetlik, W., and McGuire, C.: Soil Survey of Walnut Gulch Experimental Watershed, Arizona, Tucson, AZ: USDA-SCS and USDA-ARS in cooperation with Arizona Agricultural Experiment Station, 1993.

Brown, M., Black, E., Asfaw, D., and Otu-Larbi, F.: Monitoring drought in Ghana using TAMSAT-ALERT: a new decision support system, Weather, 72, 201-205, 10.1002/wea.3033, 2017.

Chen, M., Willgoose, G. R., and Saco, P. M.: Spatial prediction of temporal soil moisture dynamics using HYDRUS-1D, Hydrological Processes, 28, 171-185, 10.1002/hyp.9518, 2014.

Cuthbert, M. O., Taylor, R. G., Favreau, G., Todd, M. C., Shamsudduha, M., Villholth, K. G., MacDonald, A. M., Scanlon, B. R., Kotchoni, D. O. V., Vouillamoz, J.-M., Lawson, F. M. A., Adjomayi, P. A., Kashaigili, J., Seddon, D., Sorensen, J. P. R., Ebrahim, G. Y., Owor, M., Nyenje, P. M., Nazoumou, Y., Goni, I., Ousmane, B. I., Sibanda, T., Ascott, M. J., Macdonald, D. M. J., Agyekum, W., Koussoubé, Y., Wanke, H., Kim, H., Wada, Y., Lo, M.-H., Oki, T., and Kukuric, N.: Observed controls on resilience of groundwater to climate variability in sub-Saharan Africa, Nature, 572, 230-234, 10.1038/s41586-019-1441-7, 2019.

Davenport, F. M., Harrison, L., Shukla, S., Husak, G., Funk, C., and McNally, A.: Using out-of-sample yield forecast experiments to evaluate which earth observation products best indicate end of season maize yields, Environmental Research Letters, 14, 124095, 10.1088/1748-9326/ab5ccd, 2019.

Funk, C., Peterson, P., Landsfeld, M., Pedreros, D., Verdin, J., Shukla, S., Husak, G., Rowland, J., Harrison, L., Hoell, A., and Michaelsen, J.: The climate hazards infrared precipitation with stations—a new environmental record for monitoring extremes, Scientific Data, 2, 150066, 10.1038/sdata.2015.66, 2015.

Funk, C., Shukla, S., Thiaw, W. M., Rowland, J., Hoell, A., McNally, A., Husak, G., Novella, N., Budde, M., Peters-Lidard, C., Adoum, A., Galu, G., Korecha, D., Magadzire, T., Rodriguez, M., Robjhon, M., Bekele, E., Arsenault, K., Peterson, P., Harrison, L., Fuhrman, S., Davenport, F., Landsfeld, M., Pedreros, D., Jacob, J. P., Reynolds, C., Becker-Reshef, I., and Verdin, J.: Recognizing the Famine Early Warning Systems Network: Over 30 Years of Drought Early Warning Science Advances and Partnerships Promoting Global Food Security, Bulletin of the American Meteorological Society, 100, 1011-1027, 10.1175/bams-d-17-0233.1, 2019.

Goodrich, D. C., Keefer, T. O., Unkrich, C. L., Nichols, M. H., Osborn, H. B., Stone, J. J., and Smith, J. R.: Long-term precipitation database, Walnut Gulch Experimental Watershed, Arizona, United States, Water Resour. Res., 44, n/a-n/a, 10.1029/2006WR005782, 2008.

Gruber, A., Scanlon, T., van der Schalie, R., Wagner, W., and Dorigo, W.: Evolution of the ESA CCI Soil Moisture climate data records and their underlying merging methodology, Earth Syst. Sci. Data, 11, 717-739, 10.5194/essd-11-717-2019, 2019.

Guerreiro, S. B., Fowler, H. J., Barbero, R., Westra, S., Lenderink, G., Blenkinsop, S., Lewis, E., and Li, X.-F.: Detection of continental-scale intensification of hourly rainfall extremes, Nature Climate Change, 8, 803-807, 10.1038/s41558-018-0245-3, 2018.

Harrison, L., Funk, C., and Peterson, P.: Identifying changing precipitation extremes in Sub-Saharan Africa with gauge and satellite products, Environmental Research Letters, 14, 085007, 10.1088/1748-9326/ab2cae, 2019.

Liebmann, B., Hoerling, M. P., Funk, C., Bladé, I., Dole, R. M., Allured, D., Quan, X., Pegion, P., and Eischeid, J. K.: Understanding Recent Eastern Horn of Africa Rainfall Variability and Change, J. Clim., 27, 8630-8645, 10.1175/jcli-d-13-00714.1, 2014.

Luong, T. M., Castro, C. L., Chang, H.-I., Lahmers, T., Adams, D. K., and Ochoa-Moya, C. A.: The More Extreme Nature of North American Monsoon Precipitation in the Southwestern United States as Revealed by a Historical Climatology of Simulated Severe Weather Events, Journal of Applied Meteorology and Climatology, 56, 2509-2529, 10.1175/jamc-d-16-0358.1, 2017.

Lusamba-Dikassa, P., Nsue-Milang, D., Okello, D., Ketsela, T., Sagoe-Moses, C., Lule, F., Dushimimana, A., and Mensah, P.: Framework for supporting countries to address the food crisis and malnutrition in the African region, African Journal of Food, Agriculture, Nutrition and Development, 12, 6305-6316, 2012.

Lyon, B., and DeWitt, D. G.: A recent and abrupt decline in the East African long rains, Geophys. Res. Lett., 39, doi:10.1029/2011GL050337, 2012.

Margulis, M.: Global Food Security Governance: The Committee for World Food Security, Comprehensive Framework for Action and the G8/G20, 2012.

Nicholson, S. E.: Dryland Climatology, Cambridge University Press, Cambridge, 528 pp., 2011.

Osborn, H. B., and Lane, L.: Precipitation-runoff relations for very small semiarid rangeland watersheds, Water Resour. Res., 5, 419-425, 10.1029/WR005i002p00419, 1969.

Osborn, H. B., Renard, K. G., and Simanton, J. R.: Dense networks to measure convective rainfall in the southwestern United States, Water Resour. Res., 15, 1701-1711, 10.1029/WR015i006p01701, 1979.

Pascale, S., Boos, W. R., Bordoni, S., Delworth, T. L., Kapnick, S. B., Murakami, H., Vecchi, G. A., and Zhang, W.: Weakening of the North American monsoon with global warming, Nature Clim. Change, advance online publication, 10.1038/nclimate3412 http://www.nature.com/nclimate/journal/vaop/ncurrent/abs/nclimate3412.html#supplementary-information, 2017.

Pendergrass, A. G., and Hartmann, D. L.: Changes in the Distribution of Rain Frequency and Intensity in Response to Global Warming, J. Clim., 27, 8372-8383, 10.1175/jcli-d-14-00183.1, 2014.

Renard, K. G., Nichols, M. H., Woolhiser, D. A., and Osborn, H. B.: A brief background on the U.S. Department of Agriculture Agricultural Research Service Walnut Gulch Experimental Watershed, Water Resour. Res., 44, W05S02, 10.1029/2006wr005691, 2008.

Ritchie, J. T.: Model for predicting evaporation from a row crop with incomplete cover, Water Resour. Res., 8, 1204-1213, 10.1029/WR008i005p01204, 1972.

Rosolem, R., Shuttleworth, W. J., Zreda, M., Franz, T. E., Zeng, X., and Kurc, S. A.: The Effect of Atmospheric Water Vapor on Neutron Count in the Cosmic-Ray Soil Moisture Observing System, Journal of Hydrometeorology, 14, 1659-1671, 10.1175/jhm-d-12-0120.1, 2013.

Schaap, M. G., Leij, F. J., and van Genuchten, M. T.: rosetta: a computer program for estimating soil hydraulic parameters with hierarchical pedotransfer functions, Journal of Hydrology, 251, 163-176, http://dx.doi.org/10.1016/S0022-1694(01)00466-8, 2001.

Schrön, M., Köhli, M., Scheiffele, L., Iwema, J., Bogena, H. R., Lv, L., Martini, E., Baroni, G., Rosolem, R., Weimar, J., Mai, J., Cuntz, M., Rebmann, C., Oswald, S. E., Dietrich, P., Schmidt, U., and Zacharias, S.: Improving calibration and validation of cosmic-ray neutron sensors in the light of spatial sensitivity, Hydrol. Earth Syst. Sci., 21, 5009-5030, 10.5194/hess-21-5009-2017, 2017.

Šimůnek, J., Van Genuchten, M. T., and Šejna, M.: The HYDRUS software package for simulating the two-and three-dimensional movement of water, heat, and multiple solutes in variably-saturated porous media, Technical manual, 2012.

Singer, M. B., and Michaelides, K.: Deciphering the expression of climate change within the Lower Colorado River basin by stochastic simulation of convective rainfall, Environmental Research Letters, 12, 10.1088/1748-9326/aa8e50, 2017.

Singer, M. B., Michaelides, K., and Hobley, D. E. J.: STORM 1.0: a simple, flexible, and parsimonious stochastic rainfall generator for simulating climate and climate change, Geosci. Model Dev., 11, 3713-3726, 10.5194/gmd-11-3713-2018, 2018.

Stephens, G. L., L'Ecuyer, T., Forbes, R., Gettelmen, A., Golaz, J.-C., Bodas-Salcedo, A., Suzuki, K., Gabriel, P., and Haynes, J.: Dreary state of precipitation in global models, Journal of Geophysical Research: Atmospheres, 115, 10.1029/2010jd014532, 2010.

Taylor, R. G., Todd, M. C., Kongola, L., Maurice, L., Nahozya, E., Sanga, H., and MacDonald, A. M.: Evidence of the dependence of groundwater resources on extreme rainfall in East Africa, Nature Climate Change, 3, 374, 10.1038/nclimate1731, 2013.

Trenberth, K.: Changes in precipitation with climate change, Clim. Res., 47, 123-138, 10.3354/cr00953, 2011.

Trenberth, K. E., Zhang, Y., and Gehne, M.: Intermittency in Precipitation: Duration, Frequency, Intensity, and Amounts Using Hourly Data, Journal of Hydrometeorology, 18, 1393-1412, 10.1175/jhm-d-16-0263.1, 2017.

Tuttle, S., and Salvucci, G.: Empirical evidence of contrasting soil moisture–precipitation feedbacks across the United States, Science, 352, 825-828, 10.1126/science.aaa7185, 2016.

van Genuchten, M. T.: A Closed-form Equation for Predicting the Hydraulic Conductivity of Unsaturated Soils, Soil Sci. Soc. Am. J., 44, 892-898, 10.2136/sssaj1980.03615995004400050002x, 1980.

Wainwright, J., Parsons, A. J., and Abrahams, A. D.: Plot-scale studies of vegetation, overland flow and erosion interactions: case studies from Arizona and New Mexico, Hydrological Processes, 14, 2921-2943, 10.1002/1099-1085(200011/12)14:16/17<2921::aid-hyp127>3.0.co;2-7, 2000.

Wang, P., Quinlan, P., and Tartakovsky, D. M.: Effects of spatio-temporal variability of precipitation on contaminant migration in the vadose zone, Geophys. Res. Lett., 36, 10.1029/2009gl038347, 2009.

Zreda, M., Shuttleworth, W. J., Zeng, X., Zweck, C., Desilets, D., Franz, T., and Rosolem, R.: COSMOS: the COsmic-ray Soil Moisture Observing System, Hydrol. Earth Syst. Sci., 16, 4079-4099, 10.5194/hess-16-4079-2012, 2012.